Sediment budgeting of short-term backfilling processes: The erosional collapse of a Carolingian canal construction

Johannes Schmidt,[1]* (iD) Lukas Werther,[2] (iD) Johannes Rabiger-Völlmer,[1] Franz Herzig,[3] Birgit Schneider,[1] Ulrike Werban,[4] Peter Dietrich,[4] Stefanie Berg,[5] Sven Linzen,[6] Peter Ettel[7] and Christoph Zielhofer[1]

[1] Institute of Geography, Leipzig University, Leipzig D-04103, Germany
[2] Department for Medieval Archaeology, University of Tübingen, Tübingen D-72070, Germany
[3] Bavarian State Department for Cultural Heritage BLfD, D-86672 Thierhaupten, Germany
[4] Department Monitoring and Exploration Technologies, Helmholtz Centre for Environmental Research UFZ, D-04318, Leipzig, Germany
[5] Bavarian State Department of Cultural Heritage BLfD, D-80539, Munich, Germany
[6] Leibniz Institute of Photonic Technologies IPHT, Jena D-07745, Germany
[7] Prehistory and Early History, Friedrich-Schiller University, D-07743, Jena, Germany

Correspondence to: Johannes Schmidt, Institute of Geography, Leipzig University, D-04103 Leipzig, Germany. E-mail: j.schmidt@uni-leipzig.de

ESPL

Earth Surface Processes and Landforms

ABSTRACT: Sediment budgeting concepts serve as quantification tools to decipher the erosion and accumulation processes within a catchment and help to understand these relocation processes through time. While sediment budgets are widely used in geomorphological catchment-based studies, such quantification approaches are rarely applied in geoarchaeological studies. The case of Charlemagne's summit canal (also known as Fossa Carolina) and its erosional collapse provides an example for which we can use this geomorphological concept and understand the abandonment of the Carolingian construction site. The Fossa Carolina is one of the largest hydro-engineering projects in Medieval Europe. It is situated in Southern Franconia (48.9876°N, 10.9267°E; Bavaria, southern Germany) between the Altmühl and Swabian Rezat rivers. It should have bridged the Central European watershed and connected the Rhine–Main and Danube river systems. According to our dendrochronological analyses and historical sources, the excavation and construction of the Carolingian canal took place in AD 792 and 793. Contemporary written sources describe an intense backfill of excavated sediment in autumn AD 793. This short-term erosion event has been proposed as the principal reason for the collapse and abandonment of the hydro-engineering project. We use subsurface data (drillings, archaeological excavations, and direct-push sensing) and geospatial data (a LiDAR digital terrain model (DTM), a pre-modern DTM, and a 3D model of the Fossa Carolina] for the identification and sediment budgeting of the backfills. Dendrochronological findings and radiocarbon ages of macro remains within the backfills give clear evidence for the erosional collapse of the canal project during or directly after the construction period. Moreover, our quantification approach allows the detection of the major sedimentary collapse zone. The exceedance of the manpower tipping point may have caused the abandonment of the entire construction site. The spatial distribution of the dendrochronological results indicates a north–south direction of the early medieval construction progress. © 2020 The Authors. Earth Surface Processes and Landforms published by John Wiley & Sons Ltd

KEYWORDS: Sediment budgeting; Geomorphological modelling; Backfill processes; Geoarchaeology; Fossa Carolina; Early Middle Ages; South Germany

Introduction

Quantification of sedimentary processes is a hot topic in geomorphology and geoarchaeology (Brown *et al.*, 2009; Hinderer, 2012). One of the main challenges of sediment budgeting is to quantify the sediment storage and the amount of eroded sediment (Brown *et al.*, 2009). The spatial scale of sediment budget studies can be large (e.g., the Rhine (Hoffmann *et al.*, 2007) or Mississippi river catchments (Kesel

et al., 1992)), medium (e.g., small sub-catchments (Weber and Pasternack, 2017; Rascher *et al.*, 2018)), or small (e.g., gully systems (Dotterweich *et al.*, 2003) or hillslope processes (Bussmann *et al.*, 2014; Smetanová *et al.*, 2017)). The temporal scales vary from orogenetic sediment fluxes of up to several millions of years (Hinderer and Einsele, 2001; Bhattacharya *et al.*, 2016) to short-term rainfall events (Chen *et al.*, 2018). The terms and concepts of sediment budgeting are used in both pristine (Voiculescu *et al.*, 2019) and strongly anthropogenic

influenced (Gellis *et al.*, 2017) catchments, or among them (Förster and Wunderlich, 2009). Sediment budgets can be calculated by using different data measurement approaches. Recent and subrecent sedimentary budgets can be investigated by instrumental data and monitoring approaches (Gellis *et al.*, 2017; Griffiths and Topping, 2017). Sedimentary archives such as marine deposits (Qiao *et al.*, 2017), lakes (Zolitschka, 1998; Breuer *et al.*, 2013), fluvial/alluvial sequences (Hoffmann *et al.*, 2007), deltas (Erkens *et al.*, 2006; Kondolf *et al.*, 2018), colluvial and slope deposits (Förster and Wunderlich, 2009) are used to calculate sediment budgets. However, sediment budgeting approaches are not typically applied in geoarchaeological research. Although there are studies that challenge sediment quantification in archaeological contexts (Lacquement, 2010; Sherwood and Kidder, 2011; Pickett *et al.*, 2016; Schmidt *et al.*, 2019), sediment budgets dealing with quantities of erosion and accumulation are sparse (Bork *et al.*, 2003).

Our study comprises sedimentary and dendroarchaeological data using a modelling approach in the context of a very well-dated archaeological site in Southern Germany. The object of our study is the Fossa Carolina, an Early Medieval canal that should have bridged the Central European Watershed (Leitholdt *et al.*, 2012). Recently, extensive research has been done on the sediments within the canal trench (Zielhofer *et al.*, 2014; Kirchner *et al.*, 2018; Völlmer *et al.*, 2018). Stratigraphic data show initial erosion of the dams, and nearly all drillings show initial sedimentary backfills at the trench bottom (Zielhofer *et al.*, 2014). To our knowledge, no published work has focused on the backfills or their value for understanding canal construction and site abandonment. Furthermore, to assess the linkage with wider landscape dynamics, we will compare the backfilling collapse with already published phases of soil erosion elsewhere (Dotterweich, 2008; Dreibrodt *et al.*, 2010) and climate reconstructions (Muigg *et al.*, 2020). Therefore, in this study, we present stratigraphic and geochemical results to identify these backfills. Three archaeological excavations in the Northern and North-Eastern Sections have revealed the status of construction at the moment of abandonment (Werther and Feiner, 2014; Werther *et al.*, 2015) and several oak timbers were recovered (Werther *et al.*, 2020). Furthermore, we compile the radiocarbon ages

of the backfills, and we determine the spatial distribution of dendrochronological data from the Early Medieval canal construction. Following the modelling approach of Schmidt *et al.* (2019), we use the spatial data of the backfills and set up a quantitative model of the backfill sediment budget and, subsequently, of the collapse of the Early Medieval canal construction.

The main objectives of this study were:

- the identification of the backfill sediments and their spatial distribution;
- the development of a sediment budgeting model for the short-term backfilling processes;
- the creation of a spatiotemporal model of the canal construction and abandonment progress.

Fossa Carolina and its geographical setting

The Central European watershed divides the Rhine–Main catchment and the Danube catchment. At the Fossa Carolina, it divides the Altmühl catchment (Danube drainage system) from the Swabian Rezat catchment (Rhine–Main drainage system). According to historical sources, the Fossa Carolina was built in AD 792/793 on a valley watershed (Figure 1) and according to the revised version of the Royal Frankish Annals its termination ought to have been caused, among other things, by heavy rainfall, which induced intense erosional processes of the construction earthwork (Hack, 2014; Nelson, 2015; Werther *et al.*, 2020). 'For because of the continual rain and the bogginess of the land which was in the nature of things completely waterlogged, the work that was being done could not hold firm, given the excessive wetness, and as much of the earth as was excavated by the diggers during the day slid back again and sank into the soil during the night' (translation of the revised version to the year 793, after Nelson, 2015).

The surrounding escarpment landscape is built up by Middle to Upper Jurassic rocks (mudstones, sandstones, marl, and limestones). The valley and the valley watershed are built up by sandy to loamy, fluvial sediments of Pleistocene age with a slight Loess cover, especially at the lower slopes (Schmidt-Kaler, 1993; Zielhofer and Kirchner, 2014). The
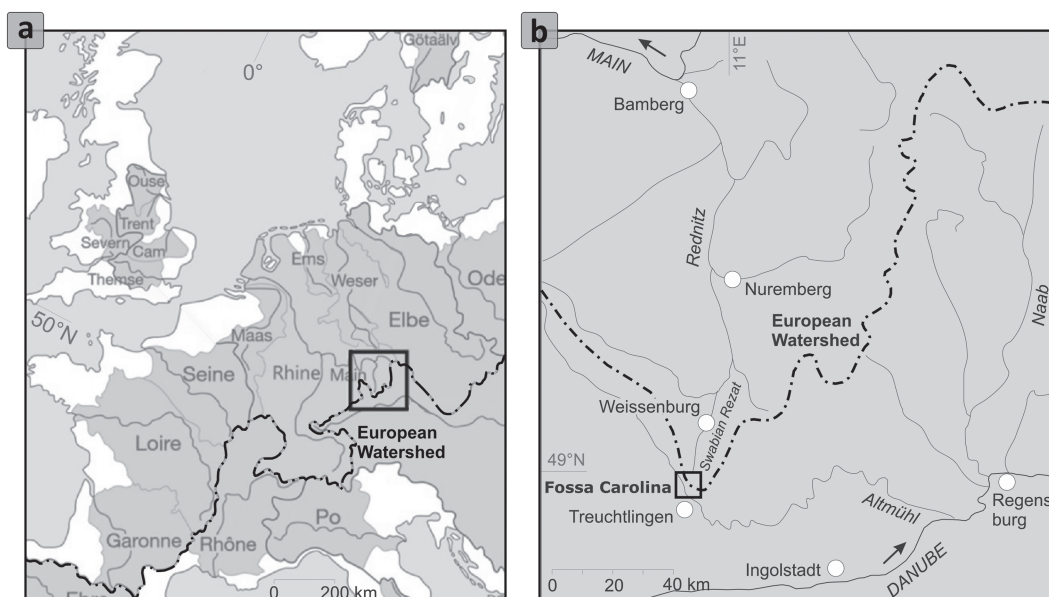
Figure 1. Geographical setting of the study area. (a) Main Central European drainage basins and the Central European Watershed. (b) Regional setting of the Fossa Carolina in relation to tributaries of the Rhine–Main drainage system and the Danube drainage system.

sediments are almost free of organic material and contain mainly fine sands (Leitholdt *et al.*, 2014; Zielhofer *et al.*, 2014). The current level of the Swabian Rezat is at 413.5 m a.s.l. and of the Altmühl River is at 408.3 m a.s.l. Because of the difference in both river levels and in order to excavate as little material as possible, the canal was set up as a summit canal (Zielhofer *et al.*, 2014). To date, no artificial inflow had been detected, and the hydroengineering approach remains unclear (Rabiger-Völlmer *et al.*, 2020). According to Kirchner *et al.* (2018) the canal construction was never finished, because canal structures are missing in the Altmühl floodplain.

Furthermore, the canal course was documented by geophysical prospections (Superconducting Quantum Interference Device (SQUID) and fluxgate magnetic, seismic profiles and geoelectric survey), aerial photography and analysis of LiDAR (Light Detection and Ranging) data (Zielhofer *et al.*, 2014; Linzen *et al.*, 2017; Köhn *et al.*, 2019; Stele *et al.*, 2019). The canal course can be divided into five sections (Figure 2) based on their specific geomorphological characteristics. The canal has a length of ~2.9 km, and the proof was done by drillings with subsequent sediment analyses (Leitholdt *et al.*, 2014; Zielhofer *et al.*, 2014; Kirchner *et al.*, 2018), direct push sensing (Hausmann *et al.*, 2018; Völlmer *et al.*, 2018) and archaeological excavations (Werther *et al.*, 2015). The canal course has an apparent S-shape (Figure 2), which is the best alignment in relation to the minimal excavation workload and avoidance of unfavourable site conditions, such as wet areas and unstable organic-rich sediments (Schmidt *et al.*, 2018). Therefore, the S-shape (Figure 3a,b) is a result of the impressive knowledge

of the Carolingian constructors. In total, the Carolingian workers excavated almost 300000 m³ of material and raised two surrounding dams (Schmidt *et al.*, 2019).

The canal trench has now been refilled and the canal is only slightly visible in the Northern and North-Eastern sections. However, the canal is clearly visible in the Central and West–East sections (due to the remains of dams taller than 10 m in height), but the canal trench bottom has been raised by sediment accumulation and formation of organic-rich peat layers up to 11 m above the Carolingian trench bottom level. Furthermore, the dams are partly eroded, and only ~30% of the dam material still remains (Schmidt *et al.*, 2019).

Material and Methods

This section will give an overview of the data used, accuracy, modelling and budgeting approach.

Data acquisition

Data are essential for modelling approaches. In the following subsection we will therefore describe our data acquisition and data processing method.

Geodata
The largest part of the input data for the present study are geodata, processed within a GIS environment (SAGA GIS; Conrad *et al.*, 2015).
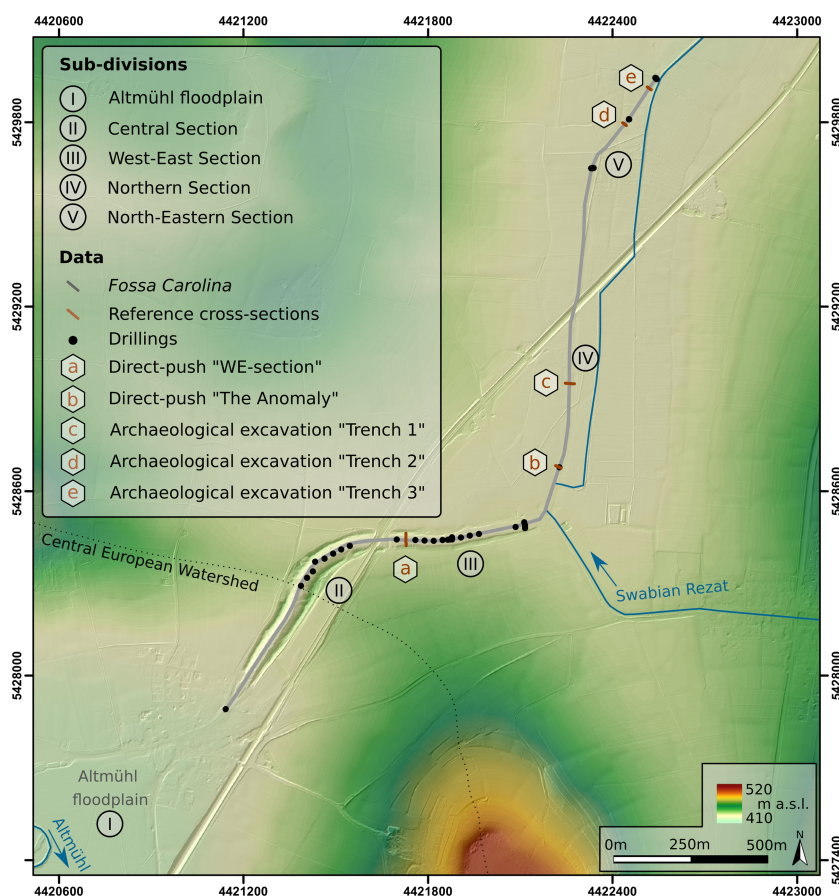
Figure 2. Local setting and course of the Fossa Carolina and its subdivisions in (I) Altmühl floodplain, (II) Central section, (III) West–East section, (IV) Northern section and (V) North-Eastern section. Direct push sensing transects (a) 'WE-section', (b) 'The Anomaly' and archaeological excavations, (c) '2013 – Trench 1', (d) '2016 – Trench 2', (e) '2016 – Trench 3'. LiDAR data were provided by the Bavarian Land Surveying Office. [Colour figure can be viewed at wileyonlinelibrary.com]
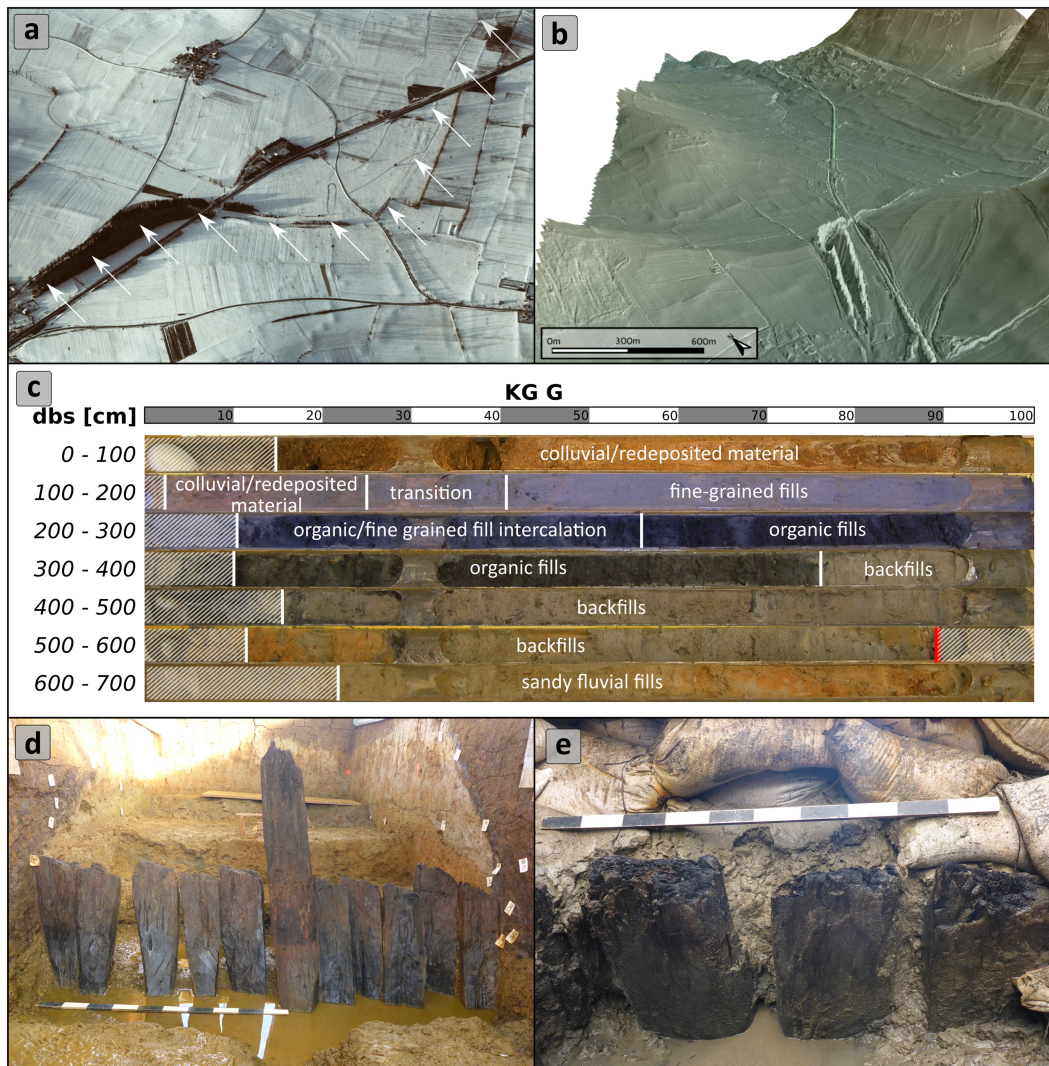
Figure 3. Impressions of the Fossa Carolina, drillings and archaeological excavation. (a) Aerial image of the canal with shadow marks highlighting terrain differences; white arrows show the canal course (Bavarian State Department of Cultural Heritage BLfD 1985). (b) 3D view of the present digital terrain model derived from LiDAR data, which show prominent dams and extent of the construction. (c) Exemplary drilling results from the Central section with stratigraphic description according to Zielhofer *et al*. (2014); the red line marks the proven trench bottom. (d) Recovered timber from trench 2 ('d' in Figure 2). (e) Recovered timber from trench 1 ('c' in Figure 2). [Colour figure can be viewed at wileyonlinelibrary.com]

LiDAR digital terrain model (DTM). We used the 1 × 1 m spatially resolved DTM, which was provided by the Bavarian Land Surveying Office (2018). It was created using high-resolution airborne laser scanning data. LiDAR DTM is a basic part of the sediment budgeting procedure.

Pre-modern DTM. The present landscape is often disturbed by anthropogenic structures, such as roads, buildings and railway tracks. We use a pre-modern DTM of the study area, where nearly all anthropogenic structures are filtered. Schmidt *et al.* (2018) removed all grid cells that were affected by anthropogenic disturbance and interpolated the residual cells to create a smooth pre-modern terrain of the study area around the Fossa Carolina. This pre-modern DTM is based on the LiDAR DTM mentioned above, and has a spatial resolution of 1 × 1 m.

3D model of the Fossa Carolina. Schmidt *et al.* (2019) developed a quantitative approach to creating a 3D model of the Fossa Carolina in its maximum state of construction. The modelling procedure was based on five reference cross-sections (archaeological excavations and direct push sensing transects) and 39 drillings. By data integration, these authors created a dense network of depth information along the canal. Owing to the high resolution of the reference

cross-sections (50 cm up to 12.5 cm), the resulting 'backfill model' has a spatial resolution of 0.5 × 0.5 m. The 3D model shows the maximum excavation depth of the Fossa Carolina. In this study, we use this information to calculate the volume of the backfill sediments and create a sediment budget.

Drillings

The basic stratigraphical data for modelling the initial backfills are the results taken from several cores (Figure 3c). The drillings were conducted during the last decade in several field campaigns. We used an Atlas Copco Cobra Pro hammer with a 60 mm open corer. For this study, we used 39 drilling cores that were situated within the trench fills (Figure 2). Subsequently, we sampled and analysed selected cores (Leitholdt *et al.*, 2014; Zielhofer *et al.*, 2014; Kirchner *et al.*, 2018).

Sediment geochemistry

We performed grain size analysis by X-ray granulometry using a SediGraph III 5120 (Micrometrics). To remove the organic matter content, we dissolved the sample in 50 mL 35% hydrogen peroxide, left it overnight, and heated the sample the next day. We added the oxidizing agent at high temperature until all organic matter was removed. Next, we dispersed the sample using 10 mL 0.4N sodium pyrophosphate solution and

ultrasonic treatment for 45 min. By wet sieving with a 63 μm sieve, the samples were separated into the sand fraction and the silt/clay fraction (<63 μm). The silt/clay fraction was analysed by means of X-ray absorption. To analyse the sand fraction, we used the dry-sieving technique. Furthermore, we calculated the organic content by measuring the total carbon content (TC) using a CNS analyser Vario EL cube (Elementar). Additionally, we determined the total inorganic carbon content (TIC) using the calcimeter technique (Scheibler method, Eijkelkamp). By subtraction, we calculated the total organic carbon content (TOC).

Radiocarbon dating

Chronological information for the backfill sediments were obtained using wood remains or charcoal material (Table I, stratigraphic positions of radiocarbon age samples can be found in supporting information Figure S1). [14]C dating was processed using accelerator mass spectrometry (AMS). We use published radiocarbon ages from Leitholdt et al. (2012) and Zielhofer et al. (2014). However, we newly calibrated all radiocarbon ages using CALIB 7.1 (Stuiver et al., 2019) with Intcal13 calibration curve (Reimer et al., 2013).

Direct push sensing

Direct push sensing is a minimally invasive and depth-accurate technique for *in situ* characterization of sediment stratigraphies (Dietrich and Leven, 2009; Leven et al., 2011). A caterpillar pushes small-diameter steel rods into the ground using various probes. We used the colour logging tool (SCOST™, Dakota Technologies, Fargo, ND, USA) to differentiate the sediment stratigraphy of the canal trench (Hausmann et al., 2018; Völlmer et al., 2018). By an appropriate measuring pace (2 cm s^{−1}) and an integration time of 300 ms, the direct push sensing results in a vertical resolution of 3 values per 2 cm. This high vertical resolution is accompanied by a horizontal spacing of up to 12.5 cm. To obtain reference cross-sections for the sediment budgeting process, we used two direct push sensing transects with 105 direct push colour logs (Figure 2).

Archaeological excavations

We conducted three archaeological excavations in 2013 and 2016 in the Northern and North-Eastern sections (Figure 2), cutting the canal rectangular to the embankments (Werther and Feiner, 2014; Werther et al., 2015, 2020; Werther, 2017). The localization of the excavation trenches was based on geoarchaeological and geophysical surveys (Linzen and Schneider, 2014; Zielhofer et al., 2014; Köhn et al., 2019). We recovered different kinds of timber and wood waste (Table II). The timbers are situated alongside the trench edges (Figure 3d,e) and stabilized the trench revetments. In this study, we use for the first time high-resolution canal trench geometries of all three trenches as cross-section reference geometries for the sediment budget calculation. Furthermore, the archaeological excavations give the chronostratigraphic context of the recovered timbers.

Dendrochronological analysis

We have used a large group of timbers and wood waste to tackle chronological questions of the canal construction. In total, 44 samples offer a reliable basis for chronological analysis (Table II). We used 30 timbers and 14 samples of wood waste with preserved terminal tree rings. Naturally, a tree forms a tree ring every year. Tree ring growth starts in spring and ends in autumn. Within this vegetation period (approximately April to September), the tree ring grows constantly. Tree growth ends with felling, and the terminal ring dates the felling date (Haneca et al., 2009). Given the seasonal information of the felling date,

Werther et al. (2020) could characterize the dendrochronological dates and discuss the construction progress at high chronological resolution. Besides the chronological information, the timbers might have marks of decay (unless they were stored in anaerobic conditions, which stops further decay) (Schweingruber, 1988). Technically, timber and wood waste were carefully cleaned and prepared to preserve all processing traces. Subsequently, tree ring widths were measured with an accuracy of 1/100 mm using a stereoscopic microscope (Herzig, 2018).

Modelling and sediment budgeting

The first challenge is the integration of all datasets to create a dense spatial network of backfill information. According to Schmidt et al. (2019), our modelling approach combines the drilling results with high-resolution cross-section reference geometries (three archaeological excavation trenches, two direct push sensing transects). For the first time, we interpolate the upper and lower limit of the backfills derived from the drillings according to the respective canal geometry. To create a dense network of depth information, we add further synthetic transects along the canal course with an equidistant spacing of ~50 m. We derived the backfill depth information from the neighbouring drillings, archaeological excavation or direct push sensing transects. We also use the respective cross-section reference geometry to interpolate the depth information on the transect. Finally, we are able to spatially interpolate all transects to generate a 3D model of the backfill top level. Similar to the 3D model with maximum excavation depth, due to the high-resolution reference cross-sections, the raster layer of the backfill sediment storage has a spatial resolution of 0.5 × 0.5 m.

Schmidt et al. (2019) recently produced a 3D model of the backfill lower level, and estimated the maximum excavation depth with the same modelling approach. Quantitatively, we applied the sediment storage of the backfills through the subtraction of both 3D models. Thus we generate a map of the spatial distribution of the backfill thickness for the entire canal. Additional separations of the backfill volumes by the main sections of the canal helps in understanding the spatial distribution of the short-term erosional process. The sediment budget is a compiled analysis of the information on maximum excavation volume, the residual dam volume and the volume of the backfill sediments. Separated by the canal sections, we can derive spatially differentiated ratios of dam erosion and backfill accumulation.

Results

Backfill sediment identification

We identified the trench bottom (lower limit of the backfills) in the drillings mainly macroscopically, because the underlying Pleistocene valley fills (Schmidt-Kaler, 1993) are almost free of organic content. However, the sedimentary material is the same in both categories. The grain size distributions of both facies are similar (e.g., sand content; Figure 4a). For a detailed sedimentary description, see Zielhofer et al. (2014). The TOC content is raised in the backfill sediments compared to the 'sterile', sandy to loamy valley fills (Figure 4b).

The lower limit in the archaeological excavation trenches was identified macroscopically while examining the total cross-section with the underlying 'natural' material and the timber. Backfills were stratigraphically identified. The high-resolution direct push sensing transects have the

Table I. Recalibrated radiocarbon ages from Zielhofer *et al.* (2014) and Leitholdt *et al.* (2014) of the backfill sediments. KIA samples were conducted at the Kiel AMS facility, SUERC samples were conducted at the Glasgow AMS facility and MAMS samples were conducted at the Mannheim AMS facility

| No.	Material	Location	Profile/core ID	Depth (level m a.s.l.)	Lab No.	^{14}C age BP (1-sigma)	Intcal13-Calibration (1sigma)	Intcal13-Calibration (2sigma)	d13C (‰)	Reference
1	charcoal	Central section	A/A26	410.9	KIA36404	1267 ± 27	689–727 737–753 757–768	666–777 793–801 844–854	−23.67 ± 0.09	Leitholdt *et al.*, 2012
2	charcoal	Central section	A/A35	409.4	KIA36406	1269 ± 27	689–725 738–768	665–776 793–800 848–851 675–778 791–828	−24.50 ± 0.14	Leitholdt *et al.*, 2012
3	wood	Central section	K/K3	413.5	SUERC-42075	1253 ± 26	691–749 761–772 778–791 804–842 860–896	838–864	−29.40	Zielhofer *et al.*, 2014
4	wood	Central section	K/K4	413.3	SUERC-42076	1163 ± 26	927–941 777–793	774–902 919–963 770–907	−27.90	Zielhofer *et al.*, 2014
5	wood	Central section	K/K5	412.9	SUERC-42140	1170 ± 34	801–893	914–968 778–790 809–813 826–841	−28.70	Zielhofer *et al.*, 2014
6	wood	Central section	L/L3	412.6	SUERC-42143	1110 ± 37	894–931 937–980 721–740 767–779	863–1,017	−27.00	Zielhofer *et al.*, 2014
7	wood	Central section	M/M2	412.9	SUERC-42148	1223 ± 37	788–873 687–725	688–888 663–777 793–802	−27.00	Zielhofer *et al.*, 2014
8	wood	West–East section	Q/Q1	412.0	SUERC-44082	1271 ± 29	738–768 664–689	844–855 660–713	−26.40	Zielhofer *et al.*, 2014
9	wood	West–East section	S/S2	412.1	MAMS 17461	1312 ± 17	752–760	744–765	−22.50	Zielhofer *et al.*, 2014

Table II. Dendrochronological results of recovered timber (oak) and wood fragments from three archaeological excavation trenches

No.	Location	Excavation year	Find label	Timber type	Felling date
1	Trench 1	2013	77	Plank	793, season unspecified
2	Trench 1	2013	81	Pile	793, ca. August–September
3	Trench 1	2013	82	Pile	793, season unspecified
4	Trench 1	2013	85	Pile	793, ca. August–September
5	Trench 1	2013	89	Pile	793, ca. August–September
6	Trench 1	2013	92	Pile	793, ca. August–September
7	Trench 1	2013	93	Pile	793, ca. August–September
8	Trench 1	2013	94	Pile	793, ca. August–September
9	Trench 2	2016	11	Pile	793, ca. April–May
10	Trench 2	2016	22	Pile	793, ca. April–May
11	Trench 2	2016	21/25	Splinter	793, ca. April–May
12	Trench 2	2016	25	Splinter	793, season unspecified
13	Trench 2	2016	25	Splinter	793, ca. April–May
14	Trench 2	2016	25	Splinter	792, season unspecified
15	Trench 2	2016	25	Splinter	793, season unspecified
16	Trench 2	2016	28	Plank	793, ca. April–May
17	Trench 2	2016	28/29	Splinter	792, season unspecified
18	Trench 2	2016	29	Splinter	793, season unspecified
19	Trench 2	2016	32	Pile	793, ca. April–May
20	Trench 2	2016	33	Pile	793, ca. April–May
21	Trench 2	2016	35	Pile	793, ca. April–May
22	Trench 2	2016	37	Pile	793, ca. April–May
23	Trench 2	2016	38	Pile	793, ca. April–May
24	Trench 2	2016	39	Pile	793, ca. April–May
25	Trench 2	2016	40	Pile	793, ca. April–May
26	Trench 2	2016	41	Pile	793, ca. April–May
27	Trench 2	2016	56	Plank	792, season unspecified
28	Trench 2	2016	80	Splinter	793, ca. April–May
29	Trench 2	2016	82	Splinter	793, ca. April–May
30	Trench 2	2016	89	Splinter	793, season unspecified
31	Trench 2	2016	88/91	Splinter	793, ca. April–May
32	Trench 2	2016	200	Forked wood	793, season unspecified
33	Trench 2	2016	203	Plank	792, ca. October–793, ca. March
34	Trench 3	2016	122	Splinter	792, season unspecified
35	Trench 3	2016	126	Wood fragment	792, season unspecified
36	Trench 3	2016	126	Pile	792, season unspecified
37	Trench 3	2016	127	Pile	793, ca. April–May
38	Trench 3	2016	128	Pile	792, ca. May–June
39	Trench 3	2016	134	Pile	792, ca. October–793, ca. March
40	Trench 3	2016	135	Plank	792, ca. October–793, ca. March
41	Trench 3	2016	140	Pile	793, ca. April–May
42	Trench 3	2016	141	Pile	792, ca. October–793, ca. March
43	Trench 3	2016	142	Pile	792, ca. October–793, ca. March
44	Trench 3	2016	143	Pile	792, ca. October–793, ca. March
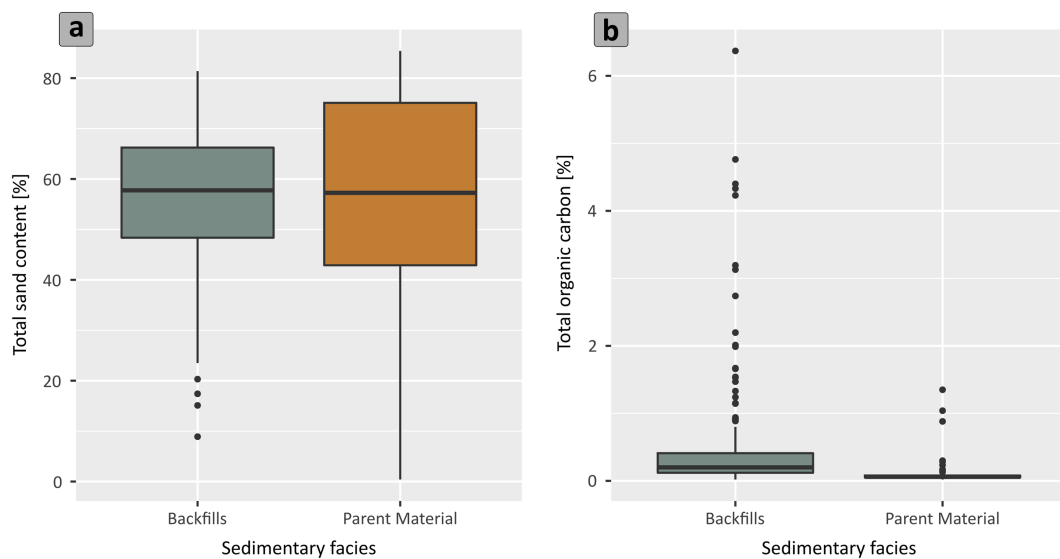
Figure 4. Summarized statistics of (a) sand content and (b) TOC content of all samples from drillings of the Fossa Carolina of the sediment facies of the 'natural, sterile parent material' and the excavated, eroded and re-accumulated backfills. [Colour figure can be viewed at wileyonlinelibrary.com]
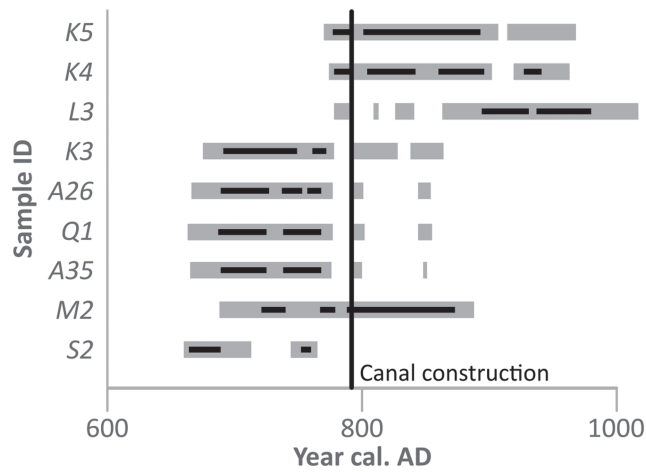
Figure 5. Calibrated radiocarbon age multiplot of the backfill sediments. Grey bars show 2-sigma ranges and black bars show 1-sigma ranges. Radiocarbon ages, newly calibrated using CALIB software (Stuiver *et al.*, 2019) with the Intcal13 calibration curve (Reimer *et al.*, 2013). The black line shows the construction of the Fossa Carolina in 792/793 AD.

advantage of also presenting the total cross-section of the canal, including the trench bottom and revetments, but with less cost and effort compared to an archaeological excavation.

The upper limit of the backfills is characterized by autochthone organic-rich sediments – mainly peat and sapropel. Therefore, the sedimentary contrast between the backfills and overlaying organic facies is very good, and detectable macroscopically in the drillings and archaeological excavations, as well as in the direct push sensing transects.

Radiocarbon results

The radiocarbon results of the backfill sediment show consistent ages (Table I; stratigraphic positions of radiocarbon samples can be found in supporting information Figure S1). All

samples are macro remains (charcoal and wood), which show, at least within their 2-sigma range ages, that fit in the time of the Fossa Carolina construction AD 792/793 (Figure 5). Within their 1-sigma range, the samples date to the construction time or before. Only sample 'S2' shows a slightly older age that does not fit in the construction time – neither within the 1-sigma nor the 2-sigma range.

Dendrochronological results

All 44 samples, which have the terminal tree ring preserved, date the tree cut-off to AD 792 or 793 (Table II). All timber in trench 1 date to AD 793, more specifically to the summer/autumn of AD 793. The results from trench 2 show mainly felling dates in spring AD 793. In trench 3, the northernmost archaeological excavation trench, the results reveal felling dates from summer AD 792 or between the growing seasons of AD 792 and 793. Most of the piles have been found *in situ*, rammed into the ground as bank revetments along the canal course. Furthermore, some planks have been found in a semi-finished condition, together with wood waste connected to the timbering on site. Most of the wood splinters belong to the final trimming of the upper parts of the piles after ramming them into the ground.

Backfill sediment storage

The sediment-storage procedure results in a map of backfill thickness covering the entire canal (Figure 6; a detailed view of backfill distribution is shown in supporting information Figure S2; detailed information concerning the backfill thickness of the drillings is summarized in supporting information Table S1). The absolute volume (~41,600 m^3) of the backfill sediments is not equally distributed along the canal. The largest proportion is localized in the Central and West–East sections. Surprisingly, the greatest thickness does not correspond to the
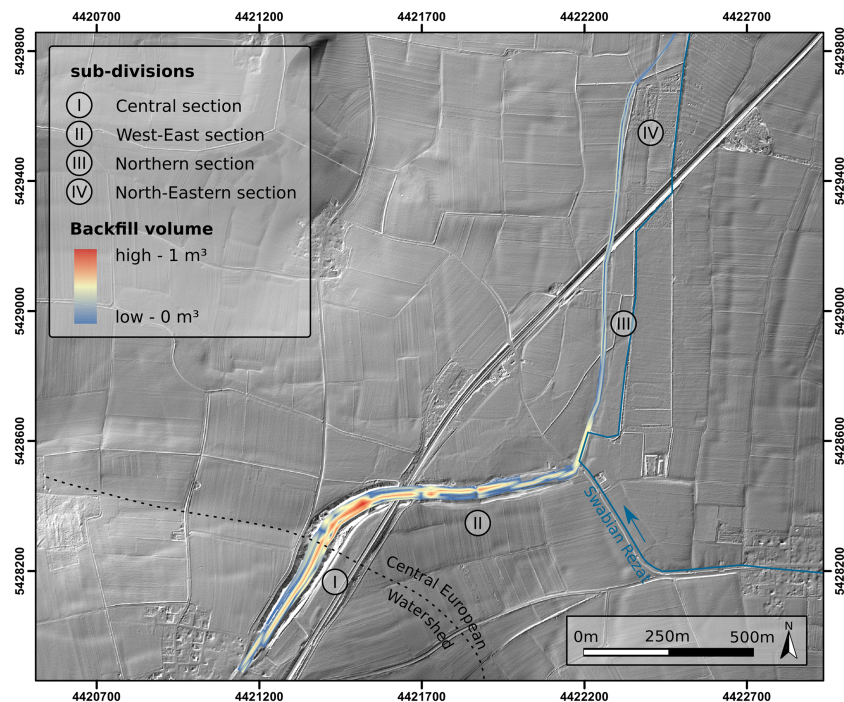
Figure 6. Spatial sediment budgeting model of the backfill thickness of the Carolingian canal Fossa Carolina. The colour ramp of the backfill volume is displayed with a gamma stretch of 2. [Colour figure can be viewed at wileyonlinelibrary.com]

Table III. Quantitative results of the sediment budgeting model of the backfill thickness and its spatial distribution for the entire canal and broken down to each canal section

	Maximum[a] (m³)	Minimum(organic fills)[b] (m³)	Initial backfills (m³)	Ratio backfill/ maximum (%)	Dams (m³)	Ratio dams/ maximum(%)	Length (m)
Total	285,455	243,820	41,635	15	119,681	42	2,829
Central section	160,815	136,379	24,436	15	85,478	53	803
WE section	84,364	74,573	9,791	12	19,268	23	494
Northern section	26,188	21,409	4,779	18	13,838	53	738
North-Eastern section	14,088	11,458	2,630	19	5,988	42	794

[a]Maximum excavation volume (from Schmidt *et al.*, 2019)
[b]Canal trench volume without backfills (bottom edge of the organic fills)

Central European watershed or, therefore, the greatest depth of excavation. It is situated ~150 m to the north.

Backfill sediment budget

The catchment of the backfill sediments is defined by the surrounding dams created by the Carolingian constructors. Hence the sediment budget is the comparison of the backfill volumes with the maximum excavation volume and the residual dam volume. Fifteen percent of the maximum excavation volume was eroded from the dams and accumulated in the canal trench (Table III). In contrast, only ~40% of the excavated material is still stored in the residual dams. Interestingly, the proportion of backfills to the maximum excavation depth over the different canal sections is similar. The ratio ranges from 12% to 19%. Surprisingly, we found the highest ratio not in the Central section, but rather in the North-Eastern section, where the lowest excavation volume occurs. In contrast, we found the lowest ratio in the West–East section. The ratio between the dams and the maximum excavation volumes is lowest in this section. Nevertheless, the total amounts of the backfill volume follow the maximum excavation volume.

Discussion

Sediment budget approach

Our sediment budgeting approach includes volume information of the maximum Carolingian excavation, present remnants of the dams and the initial backfill sediments. The quality and accuracy of the presented sediment storages at the local scale are excellent, owing to the amount of ground truth data and a reproducible modelling approach. In contrast to large-scale and catchment-based sediment budget studies (Hoffmann *et al.*, 2007), we could establish a dense network of subsurface data, but also other methodologies for the sediment storage quantification exist. Kesel (1989) used historical data to decipher the flooded areas and calculated them with mean sediment densities to estimate the sediment storage of the Mississippi River floodplain. Some studies use geostatistical interpolation of drilling results (Rommens *et al.*, 2005; Bussmann *et al.*, 2014), geometric forms of sediment bodies (derived from drillings; von Suchodoletz *et al.*, 2009), geophysical subsurface data (e.g., Guillocheau *et al.*, 2012), or isopach maps (for submarine fan or deltas; Carvajal *et al.*, 2009) to decipher the sediment storage.

Furthermore, the procedure of using synthetic transects with interpolated depth information resulted in a precise canal geometry along the entire canal course. In contrast to large-scale studies, we derived a spatially differentiated

sediment storage. In addition, we work on a small temporal scale with a short-term erosion event. Historical sources describe heavy precipitation in autumn AD 793, which caused the erosion of excavated material (Hack, 2014; Werther *et al.*, 2020). Some studies on sediment budgets struggle with the dating and methodological errors (e.g., reworked material, broad ¹⁴C range due to radiocarbon plateau, insufficient bleaching for luminescence dating) of their archives (Brown *et al.*, 2009; Bussmann *et al.*, 2014). The dendrochronological results of our study show a clear interval of the canal construction and pre-dates the accumulation of the backfills. Furthermore, the concise radiocarbon data of the backfills reveal a specific geomorphological event that occurred directly after the construction site abandonment or during the construction.

Furthermore, the biggest challenge of sediment budget studies is the estimation of sediment output. In colluvial systems (Bussmann *et al.*, 2014), fluvial systems (Förster and Wunderlich, 2009) and in deltas (Erkens *et al.*, 2006), there is an unknown proportion of sediment loss. Even though there are models available that estimate the loss, an exact estimation is crucial (Bhattacharya *et al.*, 2016). Only studies that work on continuous archives without sediment loss in endorheic geomorphological positions (sediment traps) can produce reliable information concerning sediment storage (e.g., Zolitschka, 1998; von Suchodoletz *et al.*, 2009; Breuer *et al.*, 2013). The geomorphological system of the Fossa Carolina, with its surrounding dams and excavated trench, is endorheic. Therefore, it acts solely as a sediment trap and we can assume no sediment loss of the initial backfills. Moreover, the surrounding dams form small and explicit catchments for sediment flux.

Spatial distribution of backfill sediments

Longitudinal sections of the Fossa Carolina have been published (Leitholdt *et al.*, 2012, 2014; Zielhofer *et al.*, 2014; Kirchner *et al.*, 2018), but now we are able to add two additional datasets, which concern the erosional processes during construction site abandonment (Figure 7). First, the black line shows the maximum Carolingian excavation depth, which is the result of Schmidt *et al.* (2019). Additionally, we added the orange line, which indicates the upper limit of the backfill sediments. The space between the two lines reflects the thickness of these backfill sediments. The backfill sediment thickness along the entire canal varies considerably.

The largest amounts of backfills do not correspond to the maximum excavation depth in the middle part of the Central section, as previously expected. The largest amount can be found ~150 m north of the Central European Watershed. There is a missing percentage of material in the calculation. For example, 43% of material is neither stored in the dams
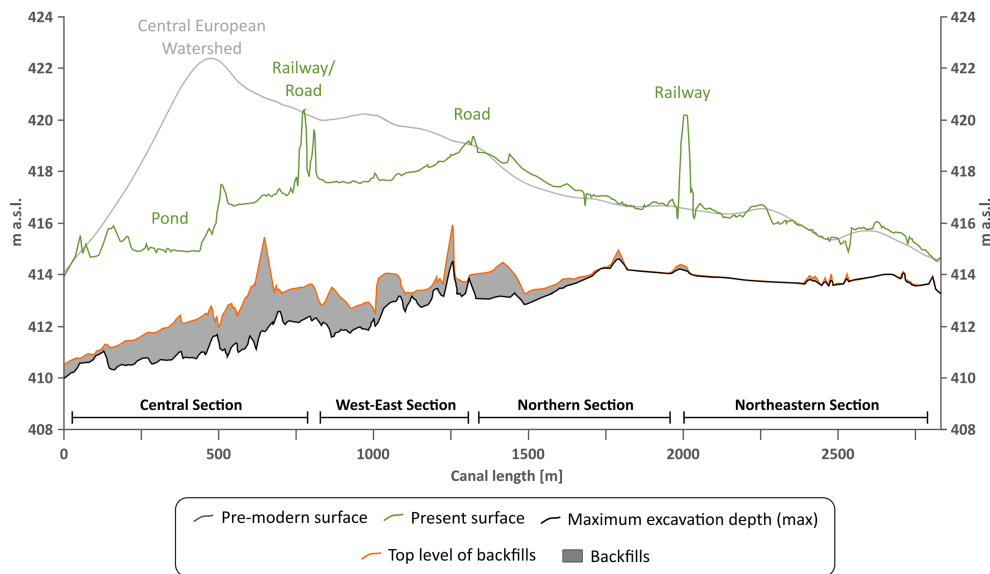
Figure 7. Canal longitudinal section with the present surface (green line; derived from the present LiDAR DTM), pre-modern surface (grey line; derived from the pre-modern DTM from Schmidt *et al.*, 2018), the maximum Carolingian excavation depth (black line, derived from the 3D-model of the Fossa Carolina from Schmidt *et al.*, 2019) and the top level of the backfills (orange line; derived from the results presented in this study). The grey area shows the thickness of the backfills for the entire Fossa Carolina. The *y*-axis is 80-fold super-elevated to show prominent information. [Colour figure can be viewed at wileyonlinelibrary.com]
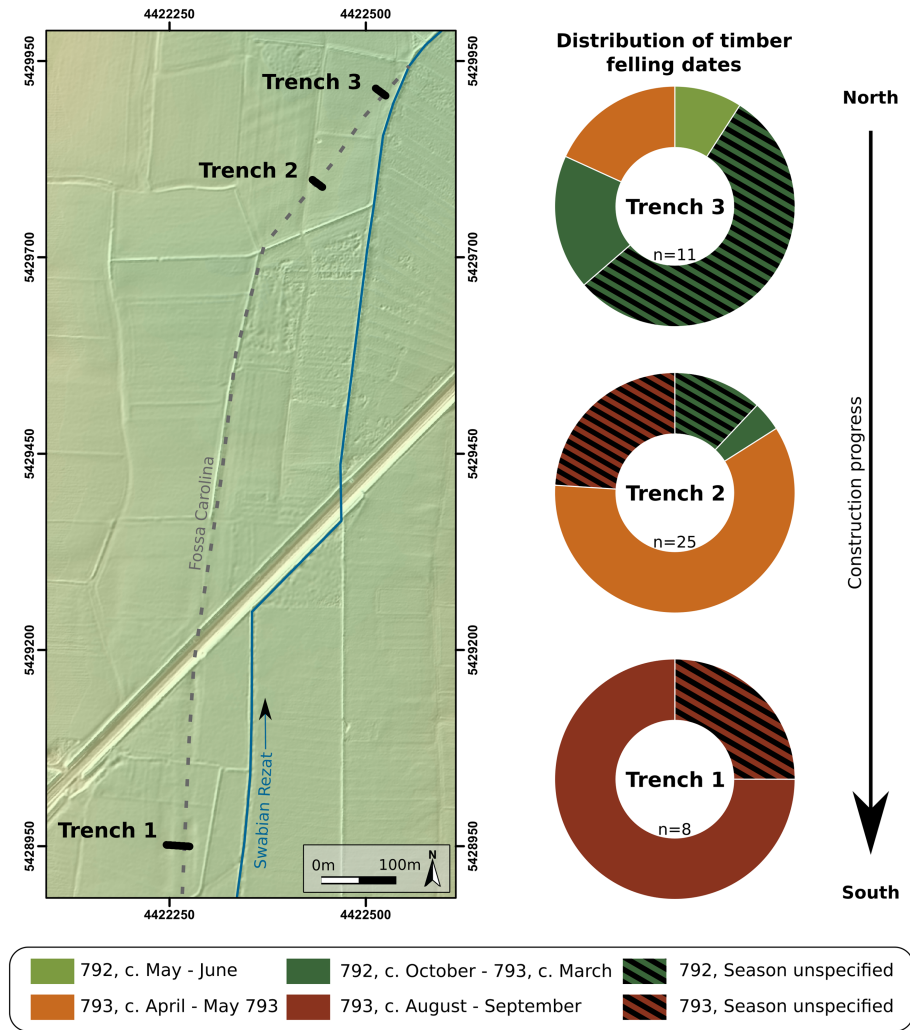
(~42%) nor backfilled (~15%) in the canal trench. The outer slopes of the dams eroded into the surrounding areas, and only the inner slopes of the dams led to the transport of material in the canal trench. One could assume the same amount of erosion to the surrounding landscape as to the canal trench. Therefore, we have a distinct 'loss' of material to the sediment cascade system of the surrounding landscape. Furthermore, during the Late Middle Ages and Early Modern time, much sediment accumulated in the upper layers of the canal trench fillings (Zielhofer *et al.*, 2014). However, there is also a strong modern anthropogenic contribution to the negative sediment balance. During railway construction, huge amounts of material have been removed from the dams in the Central section (see Schmidt *et al.*, 2018).

Canal construction progress, abandonment and collapse

Beck (1911) discussed various possibilities for the abandonment of the construction; military conflicts, subsequent food shortages, drainage problems during construction and general technical problems. Owing to the lack of subsurface data, Beck (1911) could not tackle geomorphological causality. Birzer (1998) and Koch (1993) assume the possibility of eroded dams and the redeposition of dam material within the canal trench. Nevertheless, Koch (1996) conducted drillings, but mentions the difficulties of the detection of redeposited parent material, especially without geochemical analysis or numerical dates. Our study deals with the main abandonment reason discussed in the literature: the erosional collapse of the surrounding dams. The unambiguous radiocarbon results of the backfill sediments and the stratigraphic context, directly on top of the trench bottom (precisely dated by dendrochronology), reveal the initial erosional deposition of dam material. For this study, we subdivide the construction process into two major parts: (i) the Carolingian excavation and installation of timber (the partial completion of the canal construction); and (ii) the erosional collapse and site abandonment.

i After careful consideration of the surrounding landscape, the Carolingian constructors decided to reduce the excavation volume by a topography-based S-shape canal course (Schmidt *et al.*, 2018). Within this objective, they build the canal as a summit canal (Zielhofer *et al.*, 2014). The final step of the earthwork was the installation of timber along the edges of the canal, to enhance the embankment stability (Werther *et al.*, 2015; Werther, 2016). Werther *et al.* (2020) show that all timber fellings date to AD 792 and 793. In general, the recovered timbers show almost no storage signs, such as a fungal attack. Hence we interpret the felling date as also the installation date. The spatial comparison of dendrochronological results from three archaeological excavations shows a distinct differentiation of the felling dates (Figure 8). The northernmost excavation (trench 3) reveals the oldest timber, and the excavations more to the south (trenches 2 and 1) reveal explicit younger ages. These results indicate construction progress from north to south of the canal, in the direction from the tributary to the watershed. Concerning the artificial drainage of the Carolingian construction site, dry conditions in the construction pit were obligatory and, with the north-to south approach, feasible. Kirchner *et al.* (2018) disproved the southern part of the canal in the Altmühl floodplain, and subsequently the construction was never finished in that section. Therefore, our construction progress direction is only reliable for the Northern sections of the canal.

ii The stratigraphy of nearly all drillings shows that the backfills cover the parent material. If the canal construction had been finished and no sudden collapse occurred, we would have found organic-rich sediments (e.g., peat, sapropel, finely layered sediments; Leitholdt *et al.*, 2014). The lack of evidence for Carolingian stable (open water) conditions supports the research hypothesis of an initial erosional collapse of the canal construction. Hence the precise dendrochronological results pre-date the erosional collapse. Furthermore, the sedimentary conditions (Figure 4) show that the backfills originate from the parent material from the surrounding dams. The radiocarbon results of macro remains within the backfills show Carolingian ages (Figure 5). Only sample

© 2020 The Authors. Earth Surface Processes and Landforms published by John Wiley & Sons Ltd

Earth Surf. Process. Landforms, Vol. **45**, 3449–3462 (2020)

Figure 8. Spatial distribution of dendrochronologically derived felling dates of timber from the three archaeological excavation along the Fossa Carolina. [Colour figure can be viewed at wileyonlinelibrary.com]

'S2', which has a slightly older age than the time of the Fossa Carolina construction, was specified as *Quercus* sp. (Zielhofer *et al.*, 2014). This age can be explained by reworking of older natural wood, as part of wood waste from Carolingian wood-working or even as part of a shoring system dating the inner part of an oak tree with a so-called old-wood effect. The Carolingian constructors usually used oak for timber (Werther, 2016). The scientific evidence of the sudden, colluvial collapse corresponds to the testimony of the revised version of the Frankish Annals, which describes the strong rainfalls in autumn AD 793, which, in the afternoon, washed back the material that the workers had excavated during the day (Nelson, 2015; Werther *et al.*, 2020). The results of sediment budgeting show that 15% of the total excavated material was eroded (Table III). The relative amounts of backfills are equally distributed along the canal, indicating that the collapse occurred on the whole canal structure. The highest absolute amounts of backfill can be found in the Central and West–East Section due to the maximum excavation depth. It is likely that the large amounts of backfill in these sections (~24000m³ and ~10000m³) led to an enormous additional workload for the workers, which should not be underestimated. One can argue that, in total, ~40000m³ of backfill acted as a tipping point and resulted in the abandonment of the construction, as contemporary written sources report (Hack, 2014; Nelson, 2015; Werther *et al.*, 2020).

Large-scale control or local feature?

The large amounts of sedimentary backfills accumulated in such a short time suggest a heavy precipitation event or another process that might have affected morphodynamics on a larger scale. Dotterweich (2008) and Dreibrodt *et al.* (2010) gave comprehensive overviews of historical soil erosion captured in slope, alluvial or lake deposits in Central Europe. Neither compilation identified distinct single erosion events for the Carolingian period. Even though the end of the 1st millennium AD is characterized by an increase of soil erosion (Bork *et al.*, 1998; Dreibrodt *et al.*, 2010), and a further increase in the High Middle Ages, the erosion rates and documented events are sparse. In contrast, the Merovingian land seems not to have caused enhanced soil erosion. Schreg (2014) argues that this might be due to a limited level of landscape cultivation and forest clearance. However, as our case study area was not affected by larger-scale to 'land-use changes' during the Carolingian period (the dams have a bare earth surface regardless of the land-use in the catchment), which is discussed in the geomorphological community as a major trigger on landscape activation (Kalis *et al.*, 2003; Dotterweich, 2008; Dreibrodt *et al.*, 2010), one might suggest a major precipitation event causing the erosional collapse of the Fossa Carolina.

Büntgen *et al.* (2011) propose a European-scale hydroclimate reconstruction based on tree rings. These authors reveal a slight precipitation increase after the end of the migration period and

the beginning of the Early Middle Ages. However, the large spatial-scale approach is not sufficient to cope with the Fossa Carolina collapse. A reconstruction of precipitation using tree-ring-based modelling approaches, among others, on the recovered timbers from Fossa Carolina was done by Muigg *et al.* (2020). Therefore, the reconstruction covers the study area perfectly, but oak tree ring growth is sensitive to spring to summer soil moisture (Pechtl and Land, 2019), and the data do not cover autumn precipitation (Fossa Carolina collapse is assumed to have occurred in the autumn of AD 793). However, Muigg *et al.* (2020) have not been able to identify a wet phase in the years after AD 793 when the construction was abandoned (at least not during April–August), which is in accordance with the Old World Drought Atlas (Cook *et al.*, 2015). Also, Land *et al.* (2019) reveal no distinct wet phases at the end of the 8th century and the beginning of the 9th century AD. In contrast, longer and pronounced wet phases (Büntgen *et al.*, 2011; Land *et al.*, 2019; Muigg *et al.*, 2020) in the High Medieval period significantly affected the hydrographic situation of the Fossa Carolina and led to the development of peats in the Fossa Carolina canal trench (Leitholdt *et al.*, 2014).

The excavated sediments stored in the dams during Carolingian canal construction are highly sensitive to erosion, due to the reworking and subsequent disturbance of sediment stabilizing properties (e.g., aggregates, cohesivity; see Jewell, 1963). Therefore, short-term precipitation events might have caused fast and significant erosion of the dams without affecting the soils at the larger landscape level. Also, Bork *et al.* (2003), Leopold *et al.* (2011) and Lisá *et al.* (2015) report fast redistribution events of excavated sediments, stored in dams and ditches. Jewell (1963) discusses studies where archaeological dams along ditches eroded due to steep slopes (angle of repose), bare earth surfaces and subsequent erosion susceptibility to rainfall events. Therefore, backfill sediments must be a common feature in many geoarchaeological sites with ditches and ditch-like structures.

Conclusion

Our study integrates various subsurface data (drillings, archaeological excavations, direct push sensing) and geospatial data (LiDAR DTM, pre-modern DTM, 3D model of the maximum excavation depth of the canal) to create the spatial distribution of backfill sediments at the Fossa Carolina in South Germany. Multimethod data integration for calculating the spatial distribution model of backfills was performed at high resolution. We identified these backfills stratigraphically and via geochemical analysis (mainly TOC and grain size distribution). Furthermore, radiocarbon ages of macro remains within the backfill reveal a clear Carolingian age. The chronological framework was supported by precise dendrochronological results from excavated timbers of the canal construction. Oak timber should stabilize the canal trench embankments and mark the completion of the specific section. Dendrochronological analysis proved that canal construction was done during AD 792–793.

Our modelling approach resulted in the spatial distribution of the backfill amounts. We have been able to show that erosional redeposition occurred along the whole canal trench. Furthermore, modelling reveals the quantity of initially eroded material that is now stored as backfills in the canal trench. With the information of the total excavated material and the sediment volume that remains in the present dams, we established a sediment budgeting approach. In total, 15% of the excavated material was redeposited as backfill in the canal trench. This large amount (~40000 m^3) could have acted as a tipping point to abandon the construction site, as contemporary written sources suggest. The major amounts of backfill in the Central section may have exceeded the Carolingian manpower. Additionally, this tipping point could have led to the abandonment and nonbeginning of the southernmost part of the canal (Altmühl floodplain section). However, there is no evidence for large-scale climatic control of the erosional collapse, but rather a high erosion sensitivity of the dams. Therefore, local precipitation events might have caused the backfilling processes. Additionally, we compiled the dendrochronological data with the excavation position. For the first time, we could reveal the Carolingian construction progress of the Fossa Carolina; the construction started in the northernmost section towards the Central European Watershed.

Data Availability Statement

The datasets used and/or analysed during the current study are available from the corresponding author on reasonable request.

Conflicts of Interest

The authors declare that they do not have any conflicts of interest.

References

Bavarian Land Surveying Office. 2018. Geländemodell. https://www.ldbv.bayern.de/produkte/3dprodukte/gelaende.html. [11 April 2018].

Beck F. 1911. *Der Karlsgraben: Eine historische, topographische und kritische Abhandlung.* Friedrich Kornschen Buchhandlung: Nürnberg.

Bhattacharya JP, Copeland P, Lawton TF, Holbrook J. 2016. Estimation of source area, river paleo-discharge, paleoslope, and sediment budgets of linked deep-time depositional systems and implications for hydrocarbon potential. *Earth-Science Reviews* **153**: 77–110.

Birzer F. 1998. Der Kanalbauversuch Karls des Großen. *Geologische Blätter für Nordost-Bayern und angrenzende Gebiete* **8**: 171–178.

Bork H-R, Bork H, Dalchow C, Faust B, Piorr H-P, Schatz T (eds). 1998. *Landschaftsentwicklung in Mitteleuropa: Wirkungen des Menschen auf die Landschaften.* Klett-Perthes: Gotha.

Bork H-R, Becker A, Bork H, Dotterweich M, Rasbach G, Schmidtchen G. 2003. Die Umwehrung der Römersiedlung Waldgirmes bei Wetzlar. In *Bodenbildungen, Bodenerosion und Reliefentwicklung im Mittel- und Jungholozän Deutschlands*, Bork H-R, Schmidtchen G, Dotterweich M (eds), Deutsche Akademie für Landeskunde: Leipzig; 187–194.

Breuer S, Kilian R, Baeza O, Lamy F, Arz H. 2013. Holocene denudation rates from the superhumid southernmost Chilean Patagonian

© 2020 The Authors. Earth Surface Processes and Landforms published by John Wiley & Sons Ltd

Earth Surf. Process. Landforms, Vol. **45**, 3449–3462 (2020)

Andes (53°S) deduced from lake sediment budgets. *Geomorphology* **187**: 135–152.

Brown AG, Carey C, Erkens G, Fuchs M, Hoffmann T, Macaire J-J, Moldenhauer K-M, Des Walling E. 2009. From sedimentary records to sediment budgets: Multiple approaches to catchment sediment flux. *Geomorphology* **108**(1–2): 35–47.

Büntgen U, Tegel W, Nicolussi K, McCormick M, Frank D, Trouet V, Kaplan JO, Herzig F, Heussner K-U, Wanner H, Luterbacher J, Esper J. 2011. 2500 years of European climate variability and human susceptibility. *Science (New York)* **331**(6017): 578–582.

Bussmann J, Stele A, Härtling JW, Zielhofer C, Fuchs MC. 2014. Holocene sediment dynamics in the vicinity of a Roman battlefield near Osnabrück (NW Germany). *Zeitschrift für Geomorphologie, Supplementary Issue* **58**(1): 97–117.

Carvajal C, Steel R, Petter A. 2009. Sediment supply: The main driver of shelf-margin growth. *Earth-Science Reviews* **96**(4): 221–248.

Chen C-W, Oguchi T, Hayakawa YS, Saito H, Chen H, Lin G-W, Wei L-W, Chao Y-C. 2018. Sediment yield during typhoon events in relation to landslides, rainfall, and catchment areas in Taiwan. *Geomorphology* **303**: 540–548.

Conrad O, Bechtel B, Bock M, Dietrich H, Fischer E, Gerlitz L, Wehberg J, Wichmann V, Böhner J. 2015. System for Automated Geoscientific Analyses (SAGA) v. 2.1.4. *Geoscientific Model Development* **8**(7): 1991–2007.

Cook ER, Seager R, Kushnir Y, Briffa KR, Büntgen U, Frank D *et al.* 2015. Old World megadroughts and pluvials during the Common Era. *Science Advances* **1**(10): 1–9, e1500561.

Dietrich P, Leven C. 2009. Direct push-technologies. In *Groundwater Geophysics*, Kirsch R (ed). Springer: Berlin; 347–366.

Dotterweich M. 2008. The history of soil erosion and fluvial deposits in small catchments of central Europe: deciphering the long-term interaction between humans and the environment – a review. *Geomorphology* **101**(1–2): 192–208.

Dotterweich M, Schmitt A, Schmidtchen G, Bork H-R. 2003. Quantifying historical gully erosion in northern Bavaria. *Catena* **50**(2-4): 135–150.

Dreibrodt S, Lubos C, Terhorst B, Damm B, Bork H-R. 2010. Historical soil erosion by water in Germany: scales and archives, chronology, research perspectives. *Quaternary International* **222**(1–2): 80–95.

Erkens G, Cohen KM, Gouw MJP, Middelkoop H, Hoek WZ. 2006. Holocene sediment budgets of the Rhine Delta (The Netherlands): a record of changing sediment delivery. In *Sediment Dynamics and the Hydromorphology of Fluvial Systems*.

Förster H, Wunderlich J. 2009. Holocene sediment budgets for upland catchments: The problem of soilscape model and data availability. *Catena* **77**(2): 143–149.

Gellis AC, Myers MK, Noe GB, Hupp CR, Schenk ER, Myers L. 2017. Storms, channel changes, and a sediment budget for an urban–suburban stream, Difficult Run, Virginia, USA. *Geomorphology* **278**: 128–148.

Griffiths RE, Topping DJ. 2017. Importance of measuring discharge and sediment transport in lesser tributaries when closing sediment budgets. *Geomorphology* **296**: 59–73.

Guillocheau F, Rouby D, Robin C, Helm C, Rolland N, Le Carlier de Veslud C, Braun J. 2012. Quantification and causes of the terrigeneous sediment budget at the scale of a continental margin: a new method applied to the Namibia–South Africa margin. *Basin Research* **24**(1): 3–30.

Hack A. 2014. Der Bau des Karlsgrabens nach den Schriftquellen. In *Großbaustelle 793: Das Kanalprojekt Karls des Großen zwischen Rhein und Donau*, Ettel P, Daim F, Berg-Hobohm S, Werther L, Zielhofer C (eds). Römisch-Germanischen Zentralmuseums: Mainz; 53–62.

Haneca K, Čufar K, Beeckman H. 2009. Oaks, tree-rings and wooden cultural heritage: a review of the main characteristics and applications of oak dendrochronology in Europe. *Journal of Archaeological Science* **36**(1): 1–11.

Hausmann J, Zielhofer C, Werther L, Berg-Hobohm S, Dietrich P, Heymann R, Werban U. 2018. Direct push sensing in wetland (geo)archaeology: high-resolution reconstruction of buried canal structures (Fossa Carolina, Germany). *Quaternary International* **473**: 21–36.

Herzig F. 2018. *Karlsgraben-Nordanschluss: Dendroarchäologische Untersuchungen.* Bayerisches Landesamt für Denkmalpflege: Thierhaupten; 1–30.

Hinderer M. 2012. From gullies to mountain belts: A review of sediment budgets at various scales. *Sedimentary Geology* **280**: 21–59.

Hinderer M, Einsele G. 2001. The world's large lake basins as denudation–accumulation systems and implications for their lifetimes. *Journal of Paleolimnology* **26**: 355–372.

Hoffmann T, Erkens G, Cohen KM, Houben P, Seidel J, Dikau R. 2007. Holocene floodplain sediment storage and hillslope erosion within the Rhine catchment. *The Holocene* **17**(1): 105–118.

Jewell PA. 1963. *The Experimental Earthwork on Overton Down Wiltshire 1960.* British Association for the Advancement of Science: London.

Kalis AJ, Merkt J, Wunderlich J. 2003. Environmental changes during the Holocene climatic optimum in central Europe: human impact and natural causes. *Quaternary Science Reviews* **22**(1): 33–79.

Kesel RH. 1989. The role of the Mississippi River in wetland loss in southeastern Louisiana, USA. *Environmental Geology and Water Sciences* **13**(3): 183–193.

Kesel RH, Yodis EG, McCraw DJ. 1992. An approximation of the sediment budget of the lower Mississippi River prior to major human modification. *Earth Surface Processes and Landforms* **17**: 711–722.

Kirchner A, Zielhofer C, Werther L, Schneider M, Linzen S, Wilken D *et al.* 2018. A multidisciplinary approach in wetland geoarchaeology: survey of the missing southern canal connection of the Fossa Carolina (SW Germany). *Quaternary International* **473**: 3–20.

Koch R. 1993. *Fossa Carolina: 1200 Jahre Karlsgraben.* München Bayerisches Landesamt für Denkmalpflege: München.

Koch R. 1996. Neue Beobachtungen und Forschungen zum Karlsgraben. *Jahrbuch des Historischen Vereins für Mittelfranken* **97**: 1–16.

Köhn D, Wilken D, de ND, Wunderlich T, Rabbel W, Werther L, Schmidt J, Zielhofer C, Linzen S. 2019. Comparison of time-domain SH waveform inversion strategies based on sequential low and bandpass filtered data for improved resolution in near-surface prospecting. *Journal of Applied Geophysics* **160**: 69–83.

Kondolf GM, Schmitt RJP, Carling P, Darby S, Arias M, Bizzi S *et al.* 2018. Changing sediment budget of the Mekong: Cumulative threats and management strategies for a large river basin. *Science of the Total Environment* **625**: 114–134.

Lacquement CH. 2010. Recalculating mound volume at moundville. *Southeastern Archaeology* **29**(2): 341–354.

Land A, Remmele S, Hofmann J, Reichle D, Eppli M, Zang C, Buras A, Hein S, Zimmermann R. 2019. Two millennia of Main region (southern Germany) hydroclimate variability. *Climate of the Past* **15**(5): 1677–1690.

Leitholdt E, Zielhofer C, Berg-Hobohm S, Schnabl K, Kopecky-Hermanns B, Bussmann J, Härtling JW, Reicherter K, Unger K. 2012. Fossa Carolina: the first attempt to bridge the Central European Watershed: a review, new findings, and geoarchaeological challenges. *Geoarchaeology* **27**(1): 88–104.

Leitholdt E, Krüger A, Zielhofer C. 2014. The medieval peat layer of the Fossa Carolina: evidence for bridging the Central European Watershed or climate control? *Zeitschrift für Geomorphologie, Supplementary Issue* **58**(1): 189–209.

Leopold M, Hürkamp K, Völkel J, Schmotz K. 2011. Black soils, sediments and brown calcic luvisols: a pedological description of a newly discovered neolithic ring ditch system at Stephansposching, Eastern Bavaria, Germany. *Quaternary International* **243**(2): 293–304.

Leven C, Weiß H, Vienken T, Dietrich P. 2011. Direct-Push-Technologien: Effiziente Untersuchungsmethoden für die Untergrunderkundung. *Grundwasser* **16**(4): 221–234.

Linzen S, Schneider M. 2014. Der Karlsgraben im Fokus der Geophysik. In *Großbaustelle 793: Das Kanalprojekt Karls des Großen zwischen Rhein und Donau*, Ettel P, Daim F, Berg-Hobohm S, Werther L, Zielhofer C (eds). Römisch-Germanischen Zentralmuseums: Mainz; 29–32.

Linzen S, Schneider M, Berg-Hobohm S, Werther L, Ettel P, Zielhofer C *et al.* 2017. From magnetic SQUID prospection to excavation: investigations at Fossa Carolina, Germany. In *12th International*

© 2020 The Authors. Earth Surface Processes and Landforms published by John Wiley & Sons Ltd

Earth Surf. Process. Landforms, Vol. **45**, 3449–3462 (2020)

Conference of Archaeoloigcal Prospection, Jennings B, Gaffney C, Sparrow T, Gaffney S (eds). Archaeo Press; 144–145.

Lisá L, Komoróczy B, Vlach M, Válek D, Bajer A, Kovárník J, Rajtár J, Hüssen CM, Šumberová R. 2015. How were the ditches filled? Sedimentological and micromorphological classification of formation processes within graben-like archaeological objects. *Quaternary International* **370**: 66–76.

Muigg B, Seim A, Tegel W, Werther L, Herzig F, Schmidt J, Zielhofer C, Land A, Büntgen U. 2020. Tree rings reveal dry conditions during Charlemagne's Fossa Carolina construction in 793 CE. *Quaternary Science Reviews* **227**: 1–13, 106040.

Nelson J. 2015. Evidence in question: dendrochronology and early medieval historians. In *Entre texte et histoire: études d'histoire médiévale offertes au professeur Soichi Sato*, Kano O, Lemâitre J-L (eds). Éditions de Boccard: Paris; 227–249.

Pechtl J, Land A. 2019. Tree rings as a proxy for seasonal precipitation variability and Early Neolithic settlement dynamics in Bavaria, Germany. *PloS one* **14**(1): 1–22, e0210438.

Pickett J, Schreck JS, Holod R, Rassamakin Y, Halenko O, Woodfin W. 2016. Architectural energetics for tumuli construction: the case of the medieval Chungul Kurgan on the Eurasian steppe. *Journal of Archaeological Science* **75**: 101–114.

Qiao S, Shi X, Wang G, Zhou L, Hu B, Hu L, Yang G, Liu Y, Yao Z, Liu S. 2017. Sediment accumulation and budget in the Bohai Sea, Yellow Sea and East China Sea. *Marine Geology* **390**: 270–281.

Rabiger-Völlmer J, Schmidt J, Linzen S, Schneider M, Werban U, Dietrich P, Wilken D, Wunderlich T, Fediuk A, Berg S, Werther L, Zielhofer C. 2020. Non-invasive prospection techniques and direct push sensing as high-resolution validation tools in wetland geoarchaeology: artificial water supply at a Carolingian canal in South Germany? *Journal of Applied Geophysics* **173**: 1–15, 103928.

Rascher E, Rindler R, Habersack H, Sass O. 2018. Impacts of gravel mining and renaturation measures on the sediment flux and budget in an alpine catchment (Johnsbach Valley, Austria). *Geomorphology* **318**: 404–420.

Reimer PJ, Bard E, Bayliss A, Beck JW, Blackwell PG, Ramsey CB, Buck CE et al. 2013. IntCal13 and Marine13 radiocarbon age calibration curves 0–50,000 years cal BP. *Radiocarbon* **55**(04): 1869–1887.

Rommens T, Verstraeten G, Poesen J, Govers G, van Rompaey A, Peeters I, Lang A. 2005. Soil erosion and sediment deposition in the Belgian loess belt during the Holocene: establishing a sediment budget for a small agricultural catchment. *The Holocene* **15**(7): 1032–1043.

Schmidt J, Werther L, Zielhofer C. 2018. Shaping pre-modern digital terrain models: the former topography at Charlemagne's canal construction site. *PloS one* **13**(7): 1–21, e0200167.

Schmidt J, Rabiger-Völlmer J, Werther L, Werban U, Dietrich P, Berg S et al. 2019. 3D-modelling of Charlemagne's Summit Canal (southern Germany): merging remote sensing and geoarchaeological subsurface data. *Remote Sensing* **11**(9): 1–21.

Schmidt-Kaler H. 1993. Geologie und Landschaftsentwicklung im Rezat-Altmühl Bereich. *Bau Intern Special Issue*: 8–10.

Schreg R. 2014. Uncultivated landscapes or wilderness? Early medieval land use in low mountain ranges and flood plains of Southern Germany. *Euorpean Journal of Post-Classical Archaeologies* **4**: 69–98.

Schweingruber FH. 1988. *Tree Rings: Basics and Applications of Dendrochronology*. Springer: Dordrecht.

Sherwood SC, Kidder TR. 2011. The DaVincis of dirt: geoarchaeological perspectives on Native American mound building in the Mississippi River basin. *Journal of Anthropological Archaeology* **30**(1): 69–87.

Smetanová A, Verstraeten G, Notebaert B, Dotterweich M, Létal A. 2017. Landform transformation and long-term sediment budget for a Chernozem-dominated lowland agricultural catchment. *Catena* **157**: 24–34.

Stele A, Fassbinder JWE, Härtling JW, Bussmann J, Schmidt J, Zielhofer C. 2019. Genesis of magnetic anomalies and magnetic properties of archaeological sediments in floodplain wetlands of the Fossa Carolina. *Archaeological Prospection* **4**(4): 1–11.

Stuiver M, Reimer PJ, Reimer RW. 2019. CALIB (www program). Available: http://calib.org [25 August 2010].

Voiculescu M, Ianăş A-N, Germain D. 2019. Exploring the impact of snow vole (*Chionomys nivalis*) burrowing activity in the Făgăra Mountains, Southern Carpathians (Romania): geomorphic characteristics and sediment budget. *Catena* **181**: 1–12, 104070.

Völlmer J, Zielhofer C, Hausmann J, Dietrich P, Werban U, Schmidt J, Werther L, Berg S. 2018. Minimalinvasive Direct-push Erkundung in der Feuchtboden (geo)archäologie am Beispiel des Karlsgrabens (Fossa Carolina). *Archäologisches Korrespondenzblatt* **48**(4): 577–608.

von Suchodoletz H, Faust D, Zöller L. 2009. Geomorphological investigations of sediment traps on Lanzarote (Canary Islands) as a key for the interpretation of a palaeoclimate archive off NW Africa. *Quaternary International* **196**(1-2): 44–56.

Weber MD, Pasternack GB. 2017. Valley-scale morphology drives differences in fluvial sediment budgets and incision rates during contrasting flow regimes. *Geomorphology* **288**: 39–51.

Werther L. 2016. Großbaustelle Karlsgraben: Eine Chaine opératoire für den Umgang mit der Ressource Holz in der Karolingerzeit. *Mitteilungen der Deutschen Gesellschaft für Archäologie des Mittelalters und der Neuzeit* **29**: 103–112.

Werther L. 2017. Karlsgraben doch schiffbar? Aktuelles aus der Landesarchäologie. *Archäologie in Deutschland* **5**: 41–42.

Werther L, Feiner D. 2014. Der Karlsgraben im Fokus der Archäologie. In *Großbaustelle 793: Das Kanalprojekt Karls des Großen zwischen Rhein und Donau*, Ettel P, Daim F, Berg-Hobohm S, Werther L, Zielhofer C (eds). Römisch-Germanischen Zentralmuseums: Mainz; 33–40.

Werther L, Zielhofer C, Herzig F, Leitholdt E, Schneider M, Linzen S, Berg-Hobohm S, Ettel P, Kirchner A, Dunkel S. 2015. Häfen verbinden. Neue Befunde zu Verlauf, wasserbaulichem Konzept und Verlandung des Karlsgrabens. In *Häfen im 1. Millennium AD: Bauliche Konzepte, herrschaftliche und religiöse Einflüsse*, Schmidts T, Vučetić MM (eds). Römisch-Germanischen Zentralmuseums: Mainz; 151–185.

Werther L, Nelson J, Herzig F, Schmidt J, Berg S, Ettel P, Linzen S, Zielhofer C. 2020. 792 or 793? Charlemagne's canal project: craft, nature and memory. *Early Medieval Europe* **28**: 444–465.

Zielhofer C, Kirchner A. 2014. Naturräumliche Gunstlage der Fossa Carolina. In *Großbaustelle 793: Das Kanalprojekt Karls des Großen zwischen Rhein und Donau*, Ettel P, Daim F, Berg-Hobohm S, Werther L, Zielhofer C (eds). Römisch-Germanischen Zentralmuseums: Mainz; 5–8.

Zielhofer C, Leitholdt E, Werther L, Stele A, Bussmann J, Linzen S, Schneider M, Meyer C, Berg-Hobohm S, Ettel P. 2014. Charlemagne's summit canal: an early medieval hydro-engineering project for passing the Central European Watershed. *PloS one* **9**(9): 1–20, e108194.

Zolitschka B. 1998. A 14,000 year sediment yield record from western Germany based on annually laminated lake sediments. *Geomorphology* **22**(1): 1–17.

Supporting Information

Additional supporting information may be found online in the Supporting Information section at the end of the article.

Figure S1: Stratigraphic positions of radiocarbon age samples. The cores are situated at their real level. The results of the radiocarbon sample IDs can be found in Table I in the manuscript.

Figure S2: Detailed view of the sedimentary backfill distributions along the Fossa Carolina canal course, respectively its sections. a) Northern section with gradual decrease of backfills, b) Central section with massive amounts of backfills, c) North-eastern section of the canal with least total amount of backfills, d) West–East section with moderate backfill amounts. Figure 6 in the manuscript shows the overview of this result along the whole canal course.

Table S1: Overview of specific depth information and thicknesses of the backfills along the canal trench derived from drilling, direct push sensing or archaeological excavations.

© 2020 The Authors. Earth Surface Processes and Landforms published by John Wiley & Sons Ltd

Earth Surf. Process. Landforms, Vol. **45**, 3449–3462 (2020)